E241 Advanced Fabrication laboratory Final Report

Fabrication and performance characterization of the dielectric elastomer actuators

Eunyoung Kim, Yujui Lin
Spring 2024

Mentors:
Swaroop Kommera, Michelle Rincon, Mark Zdeblick

ABSTRACT

Dielectric elastomer actuators (DEA) are stretchable actuators based on the dielectric elastomer, which enables large deformation and is a promising solution for the haptic device for wearable electronics. The DEA converts the electrostatic force to mechanical force through the Maxwell stress, where the compression and deformation of the elastomer enables in-plane or out-of-plane displacement. A significant challenge of the DEA is the actuation performance, where the displacement and actuation force are small, and a large voltage (~kV scale) is needed for the practical actuation. In this study, we investigated the impact of the electrode and elastomer material and the geometry of the DEA on the actuation performance. The fabrication process of the DEA is developed, and the experimental setup of displacement and actuation measurement is built for the performance characterization. The actuation performance from the experiment is also verified with the proposed Finite Element Analysis (FEA) model and shows good agreement.

Keywords: Dielectric elastomer actuator, electrode patterning, layered structures

Table of contents

1. Introduction

1.1. Motivation

The Dielectric Elastomer Actuator (DEA) is a soft material-based MEMS actuator. The actuation of the DEA is by coupling the electrostatic force and material deformation [1]. **Figure 1** shows the concept of the actuation mechanism of DEA. The electrostatic force by the attraction of electrodes on both sides of the polymer layer, which is made of dielectric elastomer, leads to a decreased polymer thickness [2]. The Maxwell stress determines the attraction force of the electrodes, where the dielectric constant of the elastomer is proportional to the actuation stress. The decreased thickness leads to the in-plane expansion of the polymer because of the incompressibility. By properly constraining the polymer, we can control the actuation direction and amplitude of the DEA [3-4]. DEA enables potential applications such as soft-robot [5], bio-compatible actuators for microfluidics [6], and haptic devices [7-8] that are unprecedented in the previous MEMS actuator.

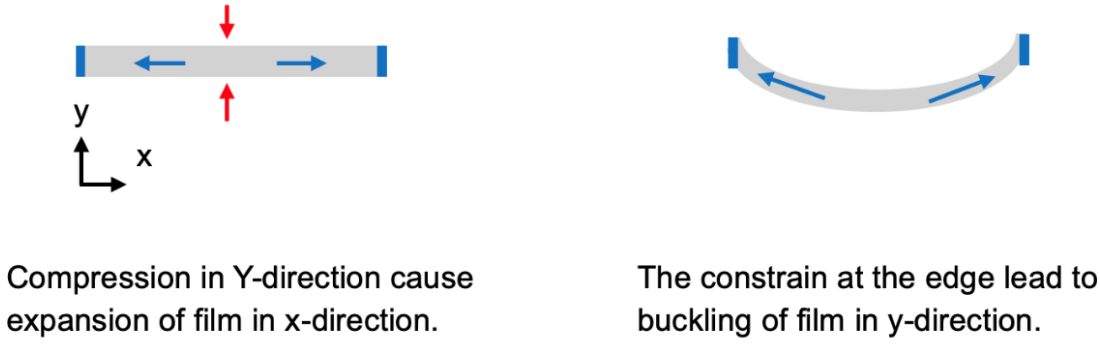

Figure 1. Schematic of the DEA actuation. (Left) The DEA film before deformation. (Right) The DEA film after the actuation, of which the out-of-plane displacement is a result of the expansion of the film.

The fabrication process of the soft material is challenging because of its difference from conventional silicon or metal-based materials. The dielectric elastomers are sensitive to organic and acid/base solvents and incompatible with the standard microfabrication process, such as the etching or lift-off process using conventional solvents. The incompatibility of soft material to the silicon-based fabrication process makes it difficult for electrode patterning. It is still not possible to optimize the performance of the DEA through the accurate modification of the electrode geometry. Additionally, the adhesion of the electrode to the elastomer is challenging and can limit actuation performance.

On the other hand, the performance characterization of the DEA is a critical issue, where the current experimental setup does not have enough time resolution to capture the displacement and force of the DEA at the higher actuation frequency (~ 10 Hz). Additionally, a reliable model to evaluate the actuation performance is still absent, and the Finite Element Analysis (FEA) simulation is desired to estimate the actuation performance before the fabrication to save time and cost.

1.2. Summary of the work

Our study proposes a fabrication method for the DEA, including the fabrication of the layered structure of the electrode and dielectric elastomer and the patterning of the electrode. The patterning process in this study modifies the conventional fabrication process that can finish in the cleanroom with the existing tools. We replaced the deposition of a hard mask on the substrate with a stencil painting using the carbon grease and stamping of the flexible electrode. The conductive polymer (PEDOT:PSS) is also investigated for the electrode material. The revised fabrication process eliminates the need to spin coat photoresist and metal lift-off, which are incompatible with the soft material. The stencil patterning process also enables an accurate definition of the geometric feature for the complicated electrode patterns on the DEA.

We also proposed the operation protocol for the performance characterization of actuation. The simulation model based on the Finite Element Analysis (FEA) is proposed and verified with the experimental results. The model provides a tool to estimate the actuation performance, including the displacement and force of the DEA based on the material properties, thickness of the layers, and electrode patterns. Additionally, we build an experimental setup for the force measurement for the DEA. The force gauge with a load cell for the actuation range of the typical DEA is set up, and the sensor is connected to the lab PC. A LabVIEW code with a high sampling rate (~100 Hz) is programmed to capture the actuation force, and the graphical user interface (GUI) makes it easier to measure and log the data through the lab PC.

1.3. Benefit to the SNF community

Our study proposed a fabrication process that is compatible with the soft material. Modifying the conventional microfabrication process enables the etching and layout patterning of the polymer structures. Also, the standardized fabrication process can expand to multi-layered structures compatible with polymer-based materials.

This study also proposed the SOP for evaluating and characterization of the actuation performance. The FEA model is proposed for the performance estimation before the fabrication, and the experimental setup for force measurement is built.

2. Fabrication process

2.1. VHB based DEA Fabrication Process

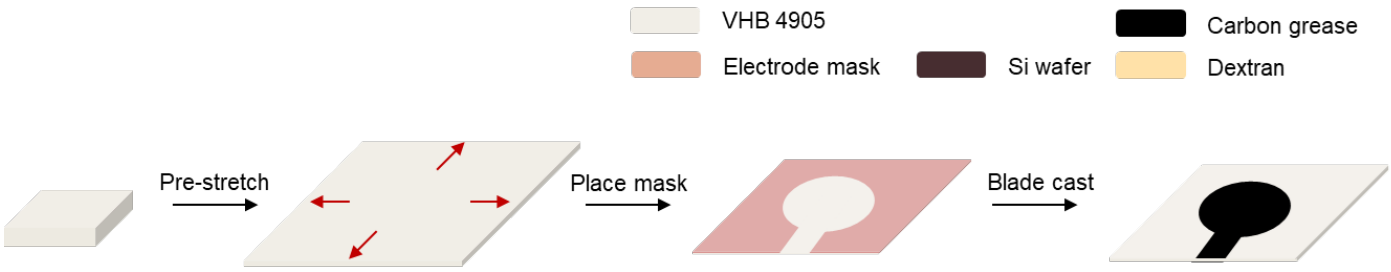

Figure 2. VHB based DEA fabrication process.

Figure 2 shows the fabrication method of VHB 4905 based DEAs. VHB 4905 is a commercially available polymer with a predefined thickness of 500 um. VHB 4905 was pre-stretched bi-axially with different ratios, then laser-cut electrode mask was placed on top and bottom of the pre-stretched VHB 4905. Carbon grease electrode was blade-casted with the designated mask shape to fabricate a DEA.

2.2 RT 601 based DEA Fabrication Process

VHB is a commercially available polymer film that has fixed thickness of 500 um. To have flexibility of being able to control the thickness of dielectric film for the future work, RT 601 was used as a spin coat-able dielectric elastomer.

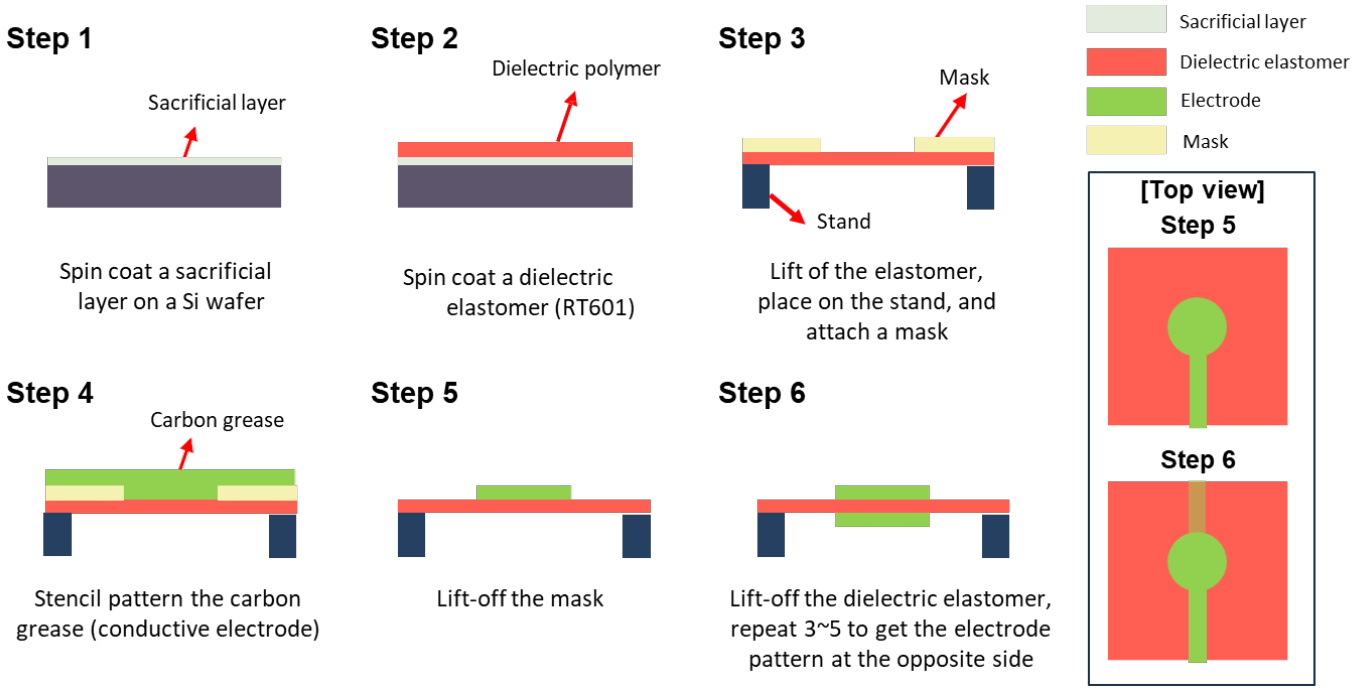

Figure 3. Fabrication process of Carbon grease/RT601 DEA.

For RT 601 based DEAs, dextran was spin coated on bare Si wafer as a sacrificial layer for the lift-off. RT 601 base and curing agent was mixed with 9:1 ratio and spin coated at 2000 rpm, then cured at 120 C for 1 hour. Dextran layer was dissolved to lift the RT 601 layer off from the Si wafer. The released RT601 was placed on a holder for blade casting. The same blade-casting method as VHB based DEAs, was used to fabricate RT 601based DEAs.

2.3 Lift off process of dielectric film

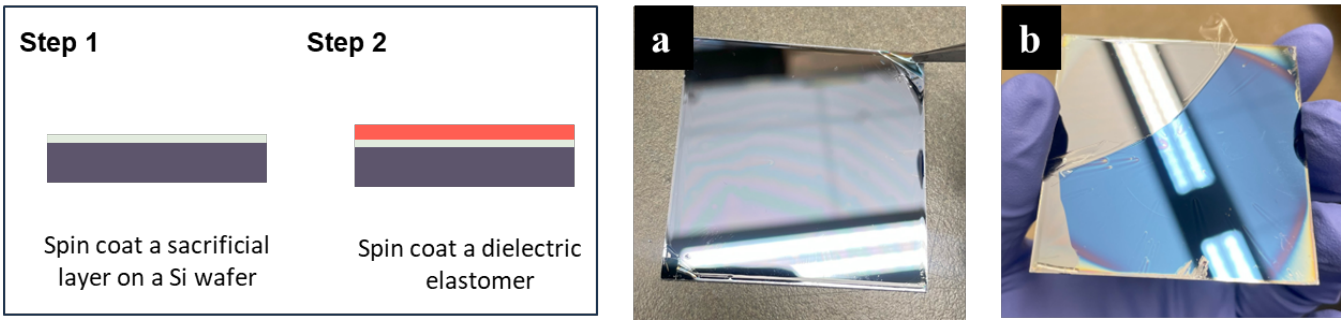

Figure 4. Attempt to peel off RT601 from Si wafer. a) before peel off, b) after peeling off.

Prior to trying the lift off process by dissolving the sacrificial layer, as it will be optimal to not involve water in the fabrication process, we tried to just peel off the dielectric elastomer from the wafer. Although out of 3 samples, one RT 601 could be peeled off in-tact, as shown in **Figure 4.b**, films broke in the middle of peeling off. Therefore, we tried to develop the lift-off process for more stable results.

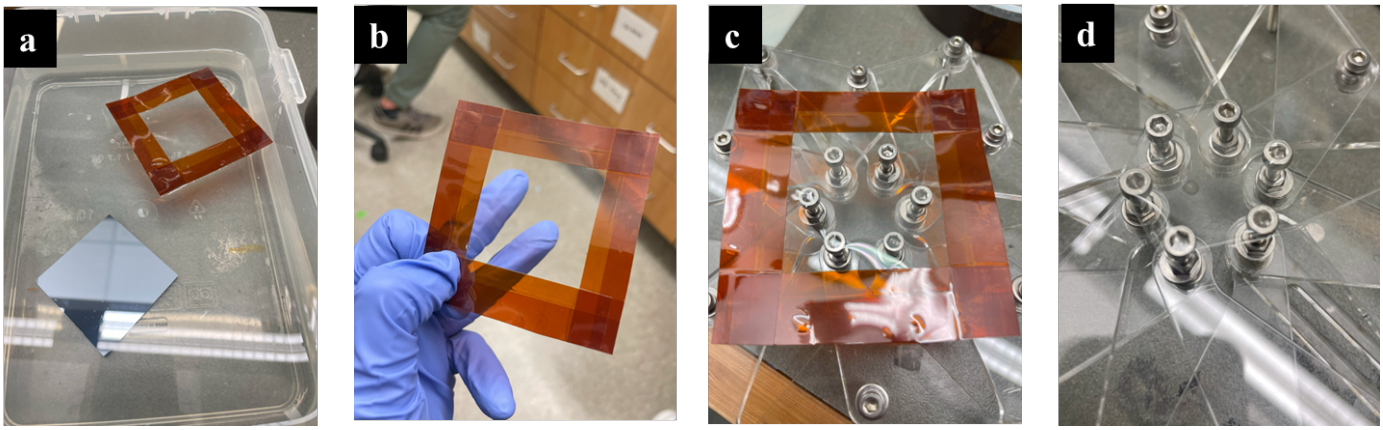

Figure 5. Successful lift off using dextran sacrificial layer. a) dissolving dextran layer to lift off the RT 601 layer with Kapton tape as a support. b) Successful lift off of RT 601 layer. c-d) placing the RT 601 layer on holder to pattern the electrode.

5 wt% dextran solution was spin coated on a bare Si wafer before spin coating RT 601. After curing the RT601 by baking at 120 C for 1 hr, Kapton tape was placed at the edge of RT 601 to serve as a support of freestanding RT 601 after the lift off. The RT601/Dextran/Si with Kapton tape support was submerged in water to dissolve the dextran sacrificial layer and the RT 601 with Kapton tape support was released as shown in **Figure 5.a** and **5.b**. The released RT601 was placed on holder to pattern the electrodes for DEA fabrication.

2.3 Patterning of the electrodes

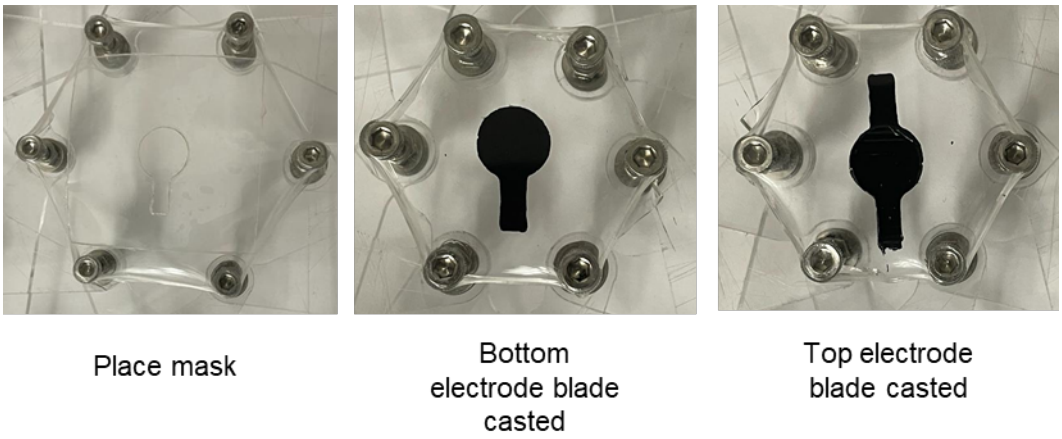

Figure 6. Carbon grease patterning with laser cut mask.

Drytac clear silicone release film was laser cut into desired electrode shape and placed on the dielectric layer as shown in **Figure 6.** Carbon grease was applied in the exposed area and blade cast to have more homogenous carbon grease pattern. The mask was peeled off after blade casting.

3. Performance characterization

3.1 The Finite Element Analysis (FEA) model

We proposed a model based on Finite Element Analysis (FEA) for the mechanical simulation of the DEA. The ABAQUS software is used for the simulation. The FEA model enables performance evaluation and parametric study before fabrication. In this project, we investigated the impact of dielectric elastomer material, the thickness of the elastomer, and the pre-stretch ratio on the out-of-plane displacement and actuation force.

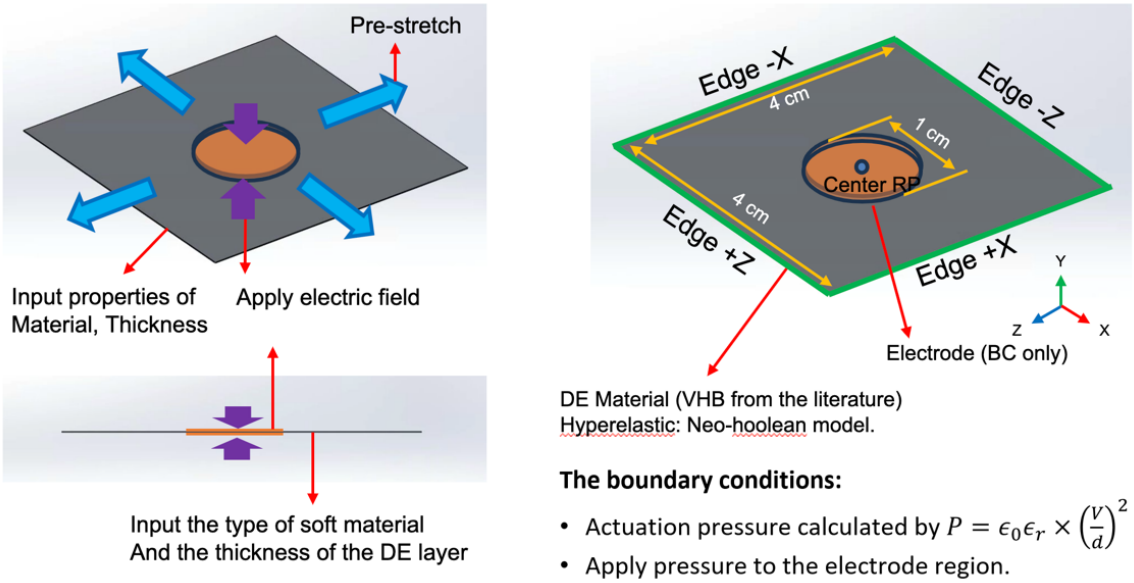

Figure 7. (Left) The boundary conditions for the pre-stretch stage. The electrostatic force is converted to the equivalent stress. (Right) The actuation stage. An initial disturbance is applied at the center to promote convergence and numerical stability.

Figure 7 shows the schematic of the boundary condition used for the FEA, where the electrodes only cover the center circle. In this project, we simplify the mechanical simulation by converting the electrostatic force to the equivalent actuation stress, P, on the electrode, where the Maxwell stress is used for the conversion:

$$P = \epsilon_0 \epsilon_r \left(\frac{V}{d}\right)^2$$

Where ϵ_0 is vacuum permeability, ϵ_r is the relativity permeability of the dielectric elastomer, V is the voltage applied to the electrode, and d is the thickness of the dielectric elastomer.

The FEA analysis for displacement modeling includes three steps during the simulation: (1) Pre-stretch, (2) Initial disturbance, and (3) Actuation of the electrode. At the pre-stretch step, we set the displacement to the four edges of the DEA, and the edge of the electrode can move freely. After pre-stretch, the four edges are fixed, so as the circumference of the electrode, to simulate the fixture of the actual experimental setup. We applied an initial disturbance before actuation of the DEA, where we set a small amount of displacement to the -Z direction at the center of the dielectric elastomer layer. The purpose of the initial disturbance is to enhance the numerical stability and promote iteration convergence. Finally, at the third step of the simulation, we applied the equivalent stress to the electrode region for the actuation. The out-of-plane displacement, which is the displacement in the -Z direction, is recorded by post-processing the FEA result.

On the other hand, the FEA analysis for the actuation force uses a boundary condition and simulation steps different from the displacement simulation. After pre-stretch, the electrode of the DEA is fixed for the actuation force simulation. This boundary condition is similar to the scenario of the experimental setup, where the DEA is in contact with the load cell and force sensor. The edge of the elastomer and the circumference of the electrode are fixed to simulate the fixture of the DEA. The block force of actuation is recorded by calculating the reaction force at the fixed electrode surface during post-processing.

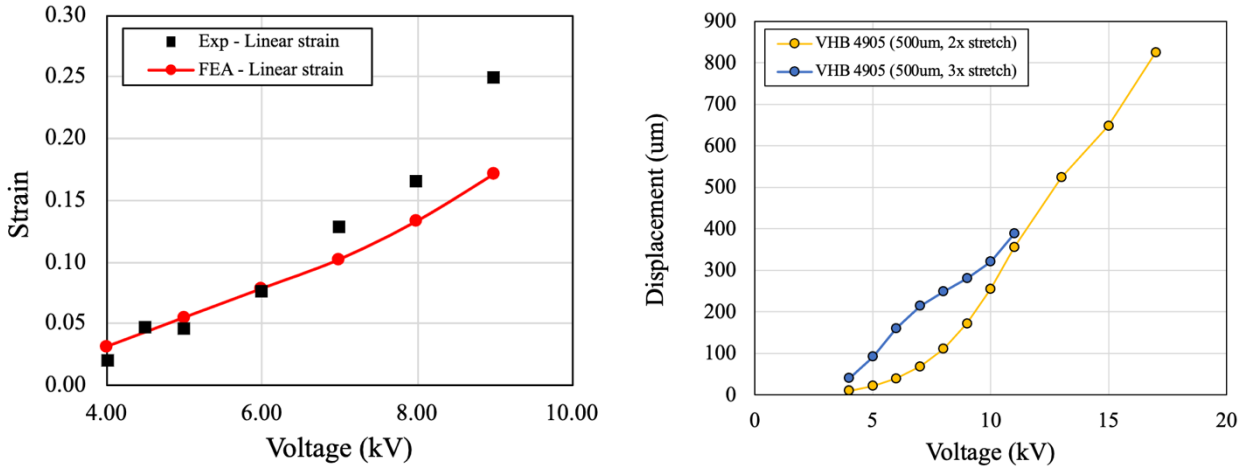

Figure 8. (Left) Verification of the simulation with the experimental data. The VHB4905 with 2x pre-stretch with investigated. (Right) Simulation result of the out-of-plane displacement for the VHB4905 DEA with different pre-stretch.

Figure 8 shows the simulation result of the DEA with VHB 4905 elastomer and the verification with the experimental data, where the result is verified with the experimental data and fits well. The result shows that a higher pre-stretch ratio leads to a higher out-of-plane displacement. Also, the thinner RT601 has a much larger displacement than the thicker VHB4905 DEAs due to the higher equivalent stress. The incompressibility indicates a thinner dielectric elastomer layer as the pre-stretch ratio increases. A higher attraction force leads to larger deformation and out-of-plane displacement.

Figure 9 replots the out-of-plane displacement to the electric field, the voltage over the elastomer thickness. The displacement from the simulation collapses into a single line in the figure. The result is reasonable as the Maxwell stress, which reflects the equivalent stress, is a function of the electric field.

The actuation force from the FEA is also in **Figure 9**, which indicates that the RT601 has a much smaller actuation force compared to VHB4905. The result shows that the thinner elastomer of the DEA can lead to a very high displacement but at the cost of a smaller actuation force. The reason is that much smaller internal stress is built in at the DEA for a thinner elastomer, which eventually leads to a smaller actuation force. Overall, the proposed simulation model verified with the experiments, provides a useful tool for evaluating the actuation performance of the DEAs.

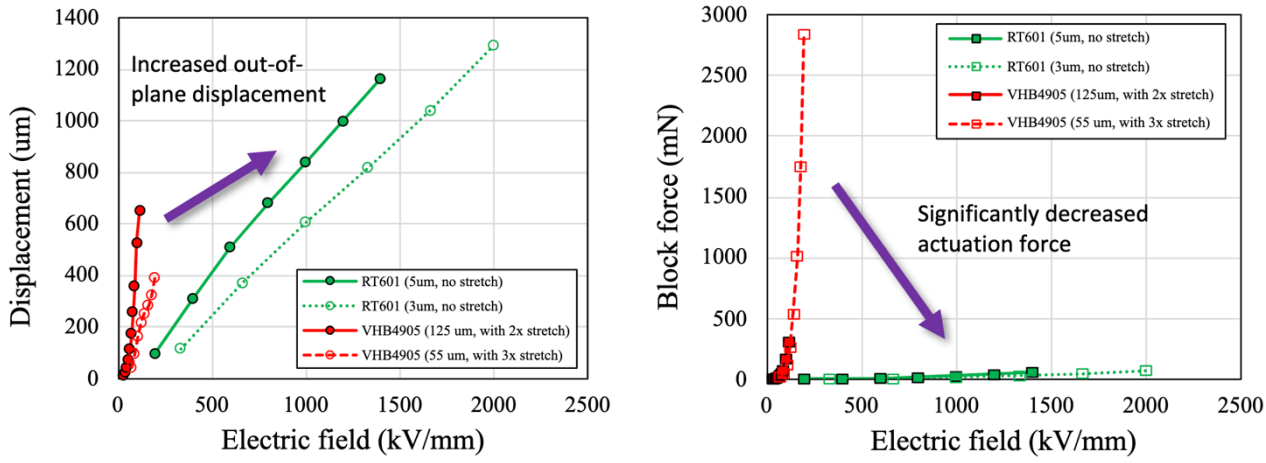

Figure 9. (Left) The out-of-plane displacement of the DEA with different elastomer material and pre-stretch ratios. The input voltage is normalized to the electric field. (Right) The actuation force at different electric field of different DEAs.

3.2 Experimental setup for the force measurement

We develop the standard operation procedure (SOP) to test the performance of DEA in this study, please refer to the SOP document. **Figure 10** shows the experimental setup for the testing of the DEA. The DEA electrodes are connected to the +V and ground. The function generator and the voltage amplifier regulate the input voltage and current. The circuit of the experimental setup includes large-Ohm electrical resistance as a safety design. The entire setup is in a safety box with 2 cm thick protective walls made of acrylic.

The actuation performance of the DEA is measured through the force sensor. The sensor is connected to the lab PC for data processing. Different pre-stretch ratios are applied with the in-house holder (**Figure 5.d**) made of laser-cut acrylic. The DEA layers are stretched at the in-plane directions before actuation to improve the stability and actuation performance due to the built-in stress and the thinner dielectric elastomer thickness.

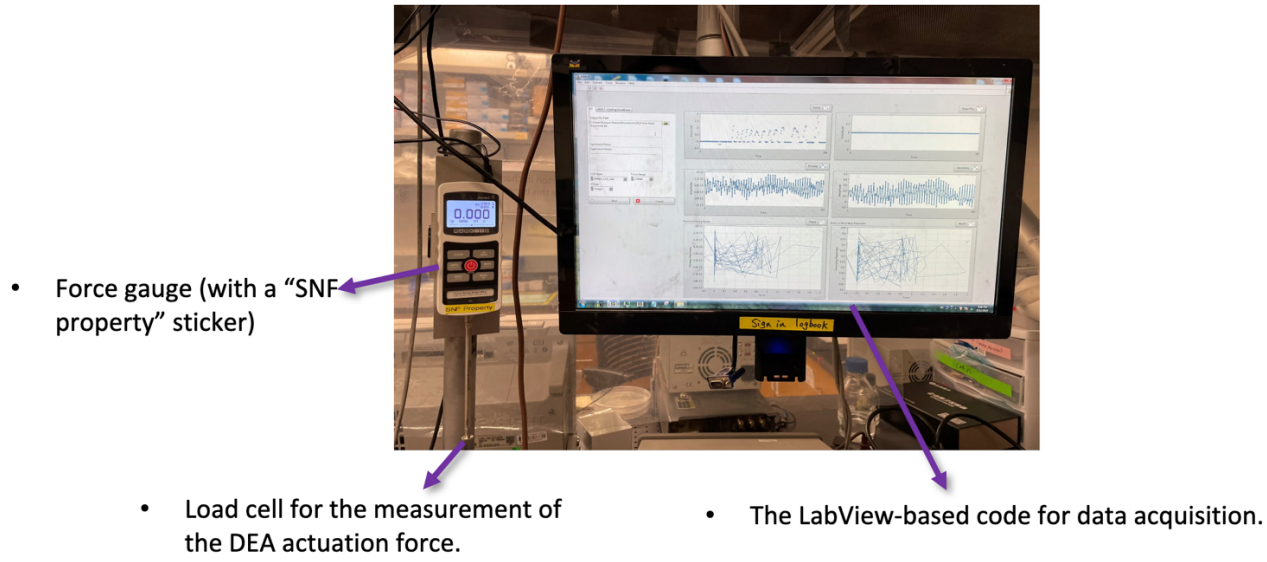

Figure 10. The experimental setup for the actuation force measurement. The DEA is contact with the force gauge during tests.

3.3 Actuation performance characterization

The actuation performances of VHB and RT601 based DEAs with different pre-stretch ratios were investigated. First, for VHB based DEAs, pre-stretch ratio of 2 and 3 were investigated, resulting in thickness of ~125 and 55 um, respectively. The actuation performances of the VHB based DEA with pre-stretching of 200 and 300% are shown in **Figure 11** and **12**, respectively. The actuation performances of RT601 based DEA without pre-stretch is also shown in **Figure 13**. In general, regardless of the material selection and pre-stretch ratio, with an increase in voltage applied to the electrodes, the actuation strain increased. The linear and areal strain were calculated using the image J and plotted. As the thicker the elastomer, more compressive force is required to actuate, to compare the actuation comparison fairly, the actuation strain was plotted against electric field, which is voltage/thickness (**Figure 14**). VHB with different pre-stretch ratios showed the similar actuation results at the same electric field, implying that the effect of pre-stretch ratios on the actuation is related to the thickness, but after eliminating the thickness effect, they will have the comparable actuation results. Therefore, to reduce the applied voltage, the thickness of the dielectric elastomer can be reduced by increasing the pre-stretch ratio. However, an optimized pre-stretch ratio should be investigated in future work, as excessive pre-stretching can lead to an earlier electric breakdown. For the RT 601, due to its stiff nature, it could not be pre-stretched and the actuation direction was in out-of-plane direction, rather than the in-plane direction that was shown in VHB based DEA. The out-of-plane displacement with increasing voltage was plotted in **Figure 14**.

At relatively low electric field (e.g. 1.5 kV), RT 601 based DEA still showed a small in-plane expansion, however, after small in-plane actuation, its expansion was constraint in the in-plane direction and started to actuate in the out-of-plane direction after 2 kV. The out-of-plane deformation could be attributed from the stiff and relatively high modulus of RT 601, constraining the in-plane expansion with the electrode area. As it serves as the constraint for the expansion, the electrode area still is subjected to expansion due to the higher electric field, therefore, the DEA actuated in out-of-plane deformation at high voltage. Therefore, depending on the application of DEA, different dielectric materials and pre-stretch ratios could be used to fit their output requirements.

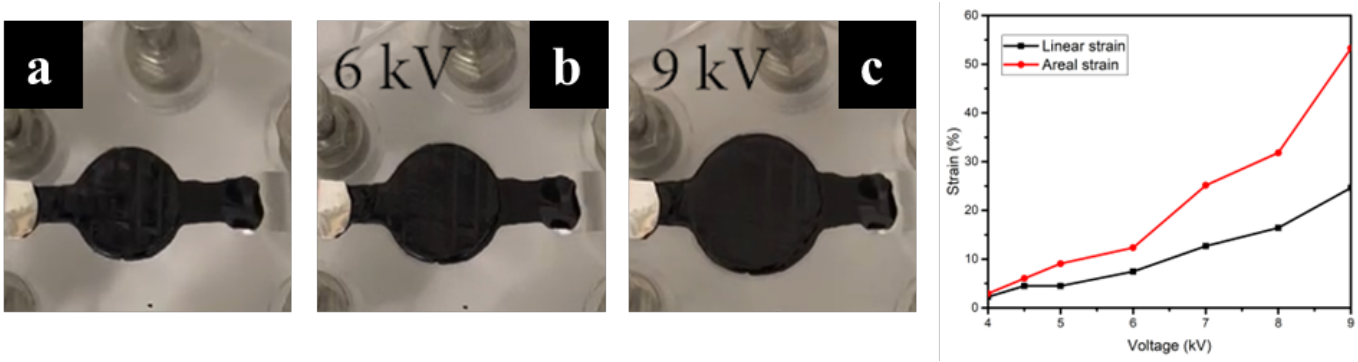

Figure 11. Actuation performance of carbon grease/VHB DEA with pre-stretch of 200%. Linear and areal strain was calculated from Carbon grease/VHB DEA with pre-stretch of 200%

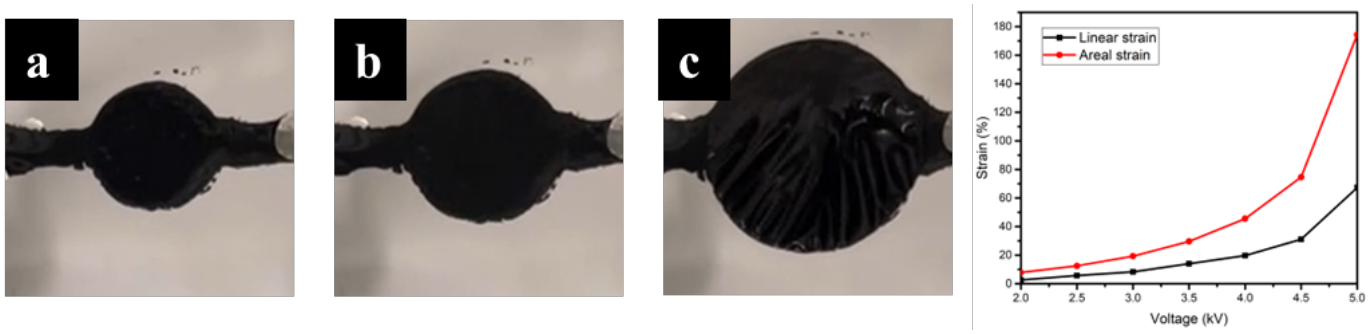

Figure 12. Actuation performance of carbon grease/VHB DEA with pre-stretch of 300%. Linear and areal strain was calculated from Carbon grease/VHB DEA with pre-stretch of 300%. a) 0 kV, b) 4 kV, and c) 5 kV.

Figure 13. Out of plane actuation of Carbon grease/RT 601 DEA without pre-stretch. Out-of-plane displacement was measured using ImageJ. a) 0 kV and b) 5 kV.

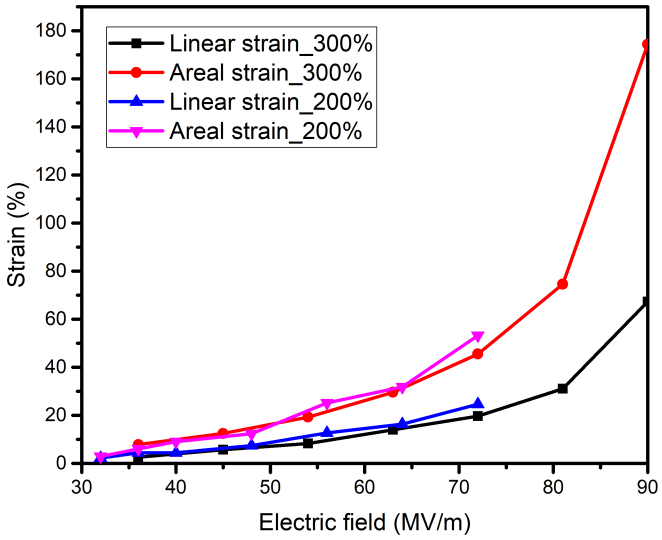

Figure 14. Strain vs Electric field comparison with different pre-stretch ratios of VHB based DEA.

4. Conclusion and Future works

We investigated the fabrication methods for the dielectric elastomer actuators (DEAs) and the impact of several design factors on the actuation performance. The difference in material properties of the polymers to the silicon makes it challenging to use the conventional fabrication method for the silicon- and metal-based materials in the fabrication of DEA. We discussed and documented different fabrication methods for the layered structure of the electrode and elastomer. Additionally, we built an experimental setup for measuring the actuation force. For the future work, the out of plane force will be characterized using the new setup. The LabVIEW code with a high sampling rate can precisely capture the dynamics of the DEA actuation. We also proposed an FEA model to evaluate the actuation force and displacement by setting different input parameters.

5. Acknowledgements

We want to thank the instructor of the E241 course, Prof. Debbie Senesky, the project mentors, Dr. Swaroop Kommera, Dr. Michelle Rincon, Dr. Mark Zdeblick, and the cohort of the E241 course, for your valuable input and feedback on the project. We would also like to thank the staff of Stanford Nanofabrication Facility (SNF), Nanopatterning Cleanroom (NPC), Hybrid Materials Facility (SMF) & Product Realization Lab (PRL) for their assistance with the tool training and fabrication process.

6. Reference

[1] E. Hajiesmaili and D. R. Clarke, “Dielectric elastomer actuators,” J. Appl. Phys., vol. 129, no. 15, Apr. 2021, doi: 10.1063/5.0043959.[1] E. Hajiesmaili and D. R. Clarke, “Dielectric elastomer actuators,” J. Appl. Phys., vol. 129, no. 15, Apr. 2021, doi: 10.1063/5.0043959.

[2] L. R. Christensen, O. Hassager, and A. L. Skov, “Electro-thermal and -mechanical model of thermal breakdown in multilayered dielectric elastomers,” *AIChE J.*, vol. 66, no. 8, Aug. 2020, doi: 10.1002/aic.16275.

[3] E. Hajiesmaili and D. R. Clarke, “Reconfigurable shape-morphing dielectric elastomers using spatially varying electric fields,” *Nat. Commun.*, vol. 10, no. 1, Dec. 2019, doi: 10.1038/s41467-018-08094-w.

[4] B. Chen *et al.*, “Design of dielectric elastomer actuators using topology optimization on electrodes,” *Smart Mater. Struct.*, vol. 29, no. 7, Jul. 2020, doi: 10.1088/1361-665X/ab8b2d.

[5] J. Phothiphatcha and T. Puttapitukporn, “Determination of material parameters of PDMS material models by MATLAB,” *Eng. J.*, vol. 25, no. 4, pp. 11–28, 2021, doi: 10.4186/ej.2021.25.4.11.

[6] F. A. Mohd Ghazali, C. K. Mah, A. AbuZaiter, P. S. Chee, and M. S. Mohamed Ali, “Soft dielectric elastomer actuator micropump,” *Sensors Actuators A Phys.*, vol. 263, pp. 276–284, Aug. 2017, doi: 10.1016/J.SNA.2017.06.018.

[7] X. Ji *et al.*, “Untethered Feel-Through Haptics Using 18-μm Thick Dielectric Elastomer Actuators,” *Adv. Funct. Mater.*, vol. 31, no. 39, pp. 1–10, 2021, doi: 10.1002/adfm.202006639.

[8] W. Qiu *et al.*, “A low voltage-powered soft electromechanical stimulation patch for haptics feedback in human-machine interfaces,” *Biosens. Bioelectron.*, vol. 193, no. June, p. 113616, 2021, doi: 10.1016/j.bios.2021.113616.